Annals of Biomedical Engineering, Vol. 38, No. 7, July 2010 *(© 2010)* pp. 2371–2382
DOI: 10.1007/s10439-010-9989-2

Electrical Impedance of Stainless Steel Needle Electrodes

HÅVARD KALVØY,[1,2] CHRISTIAN TRONSTAD,[1,2] BERNT NORDBOTTEN,[2] SVERRE GRIMNES,[1,2] and ØRJAN G. MARTINSEN[1,2]

[1]Department of Clinical and Biomedical Engineering, Rikshospitalet Oslo University Hospital, Sognsvannsveien 20, 0027 Oslo, Norway; and [2]Department of Physics, University of Oslo, Oslo, Norway

(Received 24 September 2009; accepted 24 February 2010; published online 9 March 2010)

Associate Editor Larry V. McIntire oversaw the review of this article.

Abstract—We present experimental findings regarding variability and stability of the electrical impedance properties of medical grade stainless steel needle electrodes *in vitro*. Monopolar impedance spectra (1 Hz to 1 MHz) were measured and scanning electron microscope images were obtained for five needle types with active electrode area from 0.28 to 0.7 mm^2. A saline tank (0.9% NaCl) was used as tissue model. Measurements were done before and after electrolytic treatment with anodic and cathodic DC currents of 1 μA. With active electrode areas below 1 mm^2, high influence from electrode polarization impedance (EPI) was expected at low frequencies (LF). For higher frequencies (HF) the EPI decreases and the impedance of the surrounding tissue is more pronounced. The hypothesis tested was that the EPI at LF would depend upon contact area, alloy composition, surface structure, and treatment of the active electrode, and at HF upon the electrode area geometry, and the specific resistivity of saline. Our results show large differences in electrical properties between needle types. After electrolytic treatment the EPI decreased. After 5–48 h of saline exposure the EPI increased, both for treated and untreated needles. Cathodic treatment gave lower impedance and drift than anodic or no treatment.

Keywords—Electrical properties, Medical grade, *In vitro*, EMG-electrodes, Long-term stability, SEM.

INTRODUCTION

In treatment of acute cardiac arrest, physicians need fast vascular access. In an ongoing project aiming at developing better tools for quick and effective vascular access we use medical grade stainless steel (MGSS) needle electrodes to locate the blood vessels based on impedance guided needle positioning.[15] The use of needles and other sub-mm^2 electrodes have long traditions in anesthesia,[23] neurology,[3,4] and cardiology,[24] and miniaturization of electrodes has increasing relevance in development of new applications today.[12,15,22] Clinicians and others using small electrodes for measurement or stimulation in tissue or suspension, have to take great care in using electrodes with proper characteristics. The quality and repeatability of the measurement or treatment is dependent on the electrode properties. Butson[4] concludes: "*Electrode impedance has a substantial effect on the volume of tissue activated and accurate representation of electrode impedance should be an explicit component of computational models of voltage-controlled deep brain stimulation.*" Merrill[20] has also discussed impedance and patient safety during electric stimulations. Important factors that determine the electrode properties are type of material,[21] contact area,[15] roughness factor,[1,13] geometry (Merrill *et al.*;[20] Schwan, p. 286[26]), and surface treatment[3] of the active electrode area. These factors will be the same for electrodes used both for measurements and stimulations, but the experienced impedance of the electrode system will be highly dependent of the excitation signal. For stimulation the excitation signals often are pulses driving the electrode system into non-linear operation. A typical signal can be a square pulse, which typically is monophasic with relatively high amplitude.[20] Such a signal will see a totally different impedance, compared to that measured with small signal (amplitude) sinus excitation.[8,26] In context with our application[15] the present study was limited to small signal responses due to sinus excitation within the linear region.[8,26]

Other investigators[6,8,17] have pointed out that stainless steel alloys can change electrode properties during use. Johnson *et al.*[14] have showed that the impedance of iridium microelectrodes can be reduced to less than the half after electrolytic treatment, Buchthal and Rosenfalck[3] passed current though

Address correspondence to Håvard Kalvøy, Department of Clinical and Biomedical Engineering, Rikshospitalet Oslo University Hospital, Sognsvannsveien 20, 0027 Oslo, Norway. Electronic mail: havard.kalvoy@fys.uio.no

stainless steel needle electrodes to reduce the impedance, and Wiechers *et al.*[27] have reported decreased impedance after storage in saline containing a wetting agent. In a previous study,[15] we discovered such changes in impedance after cathodic current treatment for two types of MGSS needles (types 1 and 5). To elaborate these findings and learn more about the variability in properties we here present further investigations on these needle types and three other types of commercial MGSS needle electrodes. In the previous study, we also found dominance of tissue specific properties above 10 kHz (HF). Below 10 kHz (LF) the measurements on the present needle electrodes were highly dominated by electrode polarization impedance (EPI). The change in properties after cathodic treatment was different for the two needle types. With five different needle types from four manufacturers, we could get an indication about common property variation for MGSS needle electrodes in a monopolar setup.

Our initial hypothesis was that the prospective differences in the EPI that dominated the LF impedance, would be caused by differences in active electrode area, electrolyte, alloy composition, surface structure, and treatment of the active electrode. The HF impedance was expected to be dominated by the frequency-dependent resistivity and permittivity of the tissue. If this was the case the resulting impedance could be defined by the specific impedance and the measured area of the tissue.[11] Saline (0.9% NaCl) has pure resistive properties up to very high frequencies (600 MHz)[5] and can be used as a tissue model with constant specific resistivity below such frequencies. Hence, our second hypothesis was that all differences found in saline at HF could be explained by differences in the geometry of the active electrode area.

Electrode properties were compared between new needles, after storage in saline and after different electrolytic treatments. To our knowledge such results are not sufficiently described in the literature, although they are very important for clinicians and all others using stainless steel electrodes in electrophysiology or impedance measurements.

For use in our application we needed a spatial sensitivity within a suitable range. The spatial resolution must be high enough to discriminate tissue volumes in the same range as the vessels we are looking for. But if the resolution is too high a small blood filled capillary, e.g., within a muscle volume can be misinterpreted as a vessel.

A trade off between high resolution and EPI must also be considered. In a monopolar setup the current density will be highest adjacent to the active electrode surface and fall with distance from this. Thus, the measured impedance will be dominated by the vicinity of the active electrode and reflect some kind of averaging over the tissue in this volume.[18] A smaller active electrode area will give a higher spatial resolution,[11,25] but at the same time the EPI will increase due to the inverse proportionality to the electrode radius.

While using needles we should also keep in mind that for sharp edged electrodes the shape can have large influence on the current density and how this is distributed over the electrode–tissue interface (Grimnes and Martinsen, ch. 6.3.4 & 6.3.5[11]; Woo *et al.*[28]), and that this will influence on how the sensitivity is distributed over the active electrode area.

Kalvøy *et al.*[15] showed the feasibility for discrimination of tissue using needle types 1 and 5, and the wanted spatial resolution for our application was obtained using an active electrode area of 0.3 mm^2 (needle type 1).

Stainless steel is essentially low carbon steel containing chromium at 10% or more by weight. Medical grade stainless steel 304 are defined by international standards as Fe, $<0.08\%$ C, 17.5–20% Cr, 8–11% Ni, $<2\%$ Mn, $<1\%$ Si, $<0.045\%$ P, and $<0.03\%$ S. As other stainless steel grades the 304 also comes in different "subgrades", e.g., 304L (low C), 304H (high C), and more specialized 304DDQ (deep drawing grade). To test our hypothesis we needed the alloy specification for our electrodes, but this was not sufficiently available for all needle types. With a Scanning Electron Microscope (SEM) we could get both high-resolution images of the surface structure, and estimate the alloy composition in a back scattering analysis.

At this stage of the project, we have examined the differences in commercial available MGSS electrodes. The results from this study will be used to find the best suited needle electrode for further development of our application.

MATERIALS AND METHODS

Needles

In this study we used five commercial types of insulated needle electrodes (active electrode). The needles were insulated except for the active electrode area determined by the exposed tip. Needle types 1, 2, 3, and 4 were solid with conical tip (Figs. 4–7), and type 5 was hollow with a bevel tip (Fig. 8). All needle manufacturers (distributors) were through email correspondence asked to define the type of material used (steel and insulation) and if any surface treatment was done to the active electrode area. All manufacturers specified the use of "Medical Grade Stainless Steel" (MGSS) and some also specified the AISI-grade (American iron and steel institute, all of these were 304). The insulation of needle types 1, 2, 3, and 4 was

TABLE 1. Needle types used in the present study.

Type	Name	Company	Length × diam. (mm)	Active area (mm^2)
1	Disposable monopolar needle electrode	Medtronic Inc., Minneapolis US	37 × 0.33	0.3
2	Disposable monopolar needle electrode	Medtronic Inc., Minneapolis US	50 × 0.40	0.3
3	TECA Needles disposable monopolar needle electrode	VIASYS Healthcare, Surrey UK	37 × 0.36	0.28
4	Pirouette, disposable EMG Needle	Technomed Europe, Beek Netherlands	40 × 0.35	Not given (0.5)
5	Stimuplex A	B.Braun Melsungen AG	50 × 0.7	Not given (0.7)

All needles were specified as Medical Grade Stainless Steel (MGSS). Insulation of types 1, 2, 3, and 4 was given as Teflon (not given for type 5). Needle types 4 and 5 had no given area. The area given in parenthesis is our rough estimate from measurement through a microscope and basic geometrical consideration.

given as Teflon (PTFE). No specification was given for the insulation of needle type 5. Geometrical specifications of the needle types are given in Table 1.

To investigate how the measured impedance properties were dependent on shape and surface structure of the active electrode area, SEM images with different magnification were taken of the needles. Alloy composition was also determined by using the SEM in "back scattering mode." One sample of each needle type was used for this. They were randomly picked new needles not used in any of the measurements.

Treatments

We used 21 needles of each type, in total 105 needles. The needles were organized in seven groups of three needles. Group 0 was untreated. Group −1 was given −1 μA in 1 min (the needle was connected to the negative pole of the current source for cathodic treatment), group −2 were given −1 μA in 2 min and group −3 were given 1 μA in 3 min. In the same way group 1, 2, and 3 were given +1 μA in 1, 2, and 3 min, respectively (needle connected to the positive pole for anodic treatment). All these treatments were done in a specially designed saline filled electrolytic cell (treatment cell), with similar properties as the measurement cell described in the next section. Between measurements all needles (also group 0) were kept in a saline filled storage cell with the tip and part of the insulation submerged in the saline.

Measurement Setup

All needle electrode measurements were 2-electrode (quasi-monopolar) measurements of complex impedance done with a Solartron 1260/1294-system. Frequency sweeps from 1 Hz to 1 MHz at constant voltage (30 mV rms) were performed with four frequencies/decade. With these specifications the Solartron used approximately 1.5 min for each scan. Data interpretation and presentation were done according to a series/impedance model. The measurements were

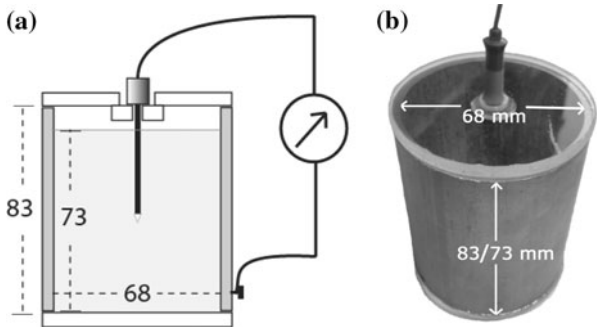

FIGURE 1. Cylindrical stainless steel measurement cell (Ø = 68 mm, height = 83 mm) filled with 73 mm saline. The upper cover contains an additional piece of Plexiglas for keeping the needle electrode in the cross-sectional center. (a) Schematic drawing; (b) Image of the used measurement cell.

done in a specially designed measurement cell (Fig. 1). This was a 83 mm high, 68 mm inner diameter, stainless steel cylinder covered with Plexiglas (5 mm thick) at both ends. By filling the cylinder with saline to a level 10 mm from the top, we had a 73 mm high cylindrical counter electrode. A hole was drilled in the Plexiglas on the top. An additional piece of Plexiglas was then mounted to support the needle in a vertical position in the cylinder. This fixed the lead connector and the first 10 mm of the needle in air. The rest of the needle length (length in Table 1 minus 10 mm) and the active electrode tip were fixed in saline in the cross-sectional center of the cylinder. The cylinder then served as a saline tank and counter electrode.

The inner diameter of 68 mm gives a counter electrode area of 15.6 cm^2. Compared to the active area of the needle electrode this was much larger, and the inside of the cylinder hence served as an Indifferent Electrode (IE). The monopolarity of the setup was tested by estimating the relative contribution from the IE on the total measured impedance. This was done by measuring the impedance of the IE in a temporary 3-electrode setup.[10] In these measurements the IE was altered to be the measured electrode. A cylindrical stainless steel current carrying (CC) electrode (approx. 3 cm^2) was added in the middle of the measurement

cell, and a cylindrical stainless steel reference electrode (approx. 0.4 cm^2) was placed in half way between the IE and the CC. Frequency sweeps showed that the IE impedance persisted below 1% of the total impedance in the initial 2-electrode setup (Fig. 1), throughout our frequency range.

All impedance measurements were done with a controlled voltage excitation signal of 30 mV rms. If the excitation voltage is chosen too high, the measurement can be done outside the linear region and the measured impedance will then be dependent on the amplitude of the excitation signal. An increased excitation signal will in that case give decreased impedance.[8,26] Sweeping the excitation amplitude during impedance measurement was done to test the linearity of our electrode/saline setup. From this pilot test we found that 30 mV was well within the linear region, and still gave measurement with very low noise.

To minimize influence from temperature drift[5,9] all measurements and storage of saline and equipment were done in controlled room temperature 23.4 ± 0.7 °C. With a temperature coefficient for saline of 2–3%/°C the error due to temperature drift would be approx. ±2%.

To avoid differences due to the filling of saline inside the different needles of type 5, all these needles were completely filled with saline and the pre-attached extension tubing was clogged by a knot to make it as short as possible.

At experiment start-up all needles were new and the sterile sealing was not broken until just before the first measurement of each needle. An initial measurement was done on all new needles. The needles in group 0 were moved directly to a saline filled tank (the storage tank) which ensured that the active electrode areas of the needles were kept in saline. All other needles were immediately after the first measurement moved to the treatment cell and given the specified electrolytic treatment. As soon as the treatment had been done each needle was moved back to the measuring cell for the second measurement (not group 0). After these initial measurements and treatments, all needles were stored in the storage tank. The total time of the measurement/treatment sequence for a needle can roughly be estimated by adding 2 min for each frequency scan to the specified treatment time (e.g., 5 min for group −1). To minimize the time between the measurements before and after treatment, each needle went through all these steps to the storage tank before the next needle was unwrapped. After 5, 24, and 48 h in the storage tank, additional measurements were done with the needles temporarily moved to the measuring cell.

RESULTS

New Needles

During the measurements on new needles, two needles of type 2 and one of type 5 temporarily lost contact in the connection lead. The same happened with one needle of type 2 during the first measurement after treatment. All these measurement are removed from the data set in all analysis. Thus, the number of needles (N) in Table 2 is not 21 for all needle types.

Student t test gave significant differences ($p < 0.001$) between all needle types at all frequencies except for the needle types 1, 2, and 3 at the two highest measurement frequencies (0.56 and 1 MHz).

The impedance spectra averaged for all new needles showed a clear increase in the modulus (Fig. 2) as the frequency decreased below 100–200 kHz for types 1 and 2, and below 10–20 kHz for needle types 3, 4, and 5. This shift along the frequency axis of about one decade for types 1 and 2 compared to the others was also seen in the phase plot (Fig. 3). This was expected since a valid measurement must follow the Kramers–Kronig relation.[11]

SEM was utilized both to provide images of different magnifications and to determine the alloy

TABLE 2. Average modulus (|Z|) and phase angle (φ) at three frequencies for all new needles sorted by needle type.

	1 MHz				10 kHz				1 Hz			
Needle type (N)	|Z| (Ω) (STD Ω/%)		φ (Deg) (STD Deg/%)		|Z| (Ω) (STD Ω/%)		φ (Deg) (STD Deg/%)		|Z| (Ω) (STD Ω/%)		φ (Deg) (STD Deg/%)	
1 (21)	312	(18/6)	−31	(3.4/11)	3551	(1059/30)	−77	(1.9/2)	7.87 M	(2.04 M/26)	−71	(1.9/3)
2 (19)	333	(40/12)	−31	(4.2/14)	2271	(882/39)	−66	(4.1/6)	3.42 M	(874 k/26)	−69	(3.3/5)
3 (21)	290	(24/8)	−22	(4.1/19)	572	(102/18)	−52	(3.0/6)	2.59 M	(555 k/21)	−80	(0.5/1)
4 (21)	173	(5,0/3)	−9	(1.7/19)	307	(51/17)	−47	(2.6/6)	765 k	(93.0 k/12)	−78	(2.0/3)
5 (20)	249	(4,5/2)	−9	(1.3/13)	432	(59/14)	−35	(3.4/10)	113 k	(49.5 k/44)	−54	(13.2/25)

Standard deviation values in ohms and percent of mean are given in parenthesis for all measurements. Number of measurements is given in parenthesis for each needle type.

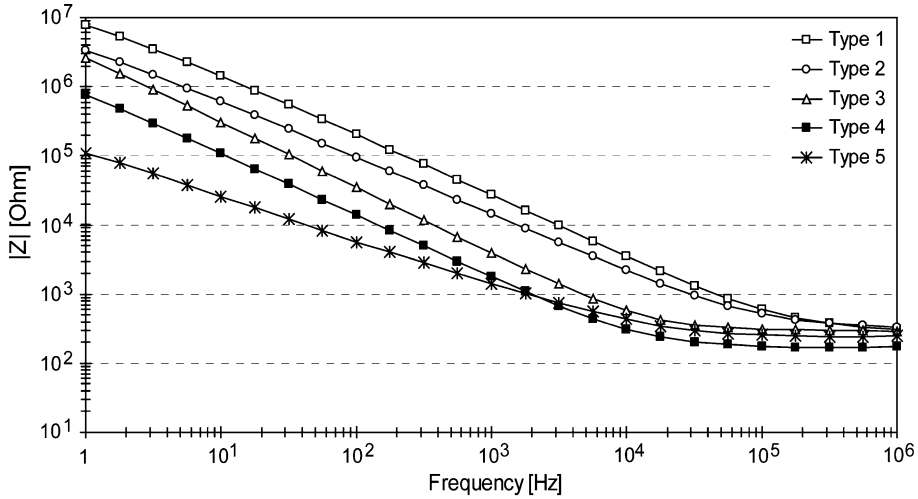

FIGURE 2. Average modulus (|*Z*|) at all measurement frequencies of all new needles sorted by needle type.

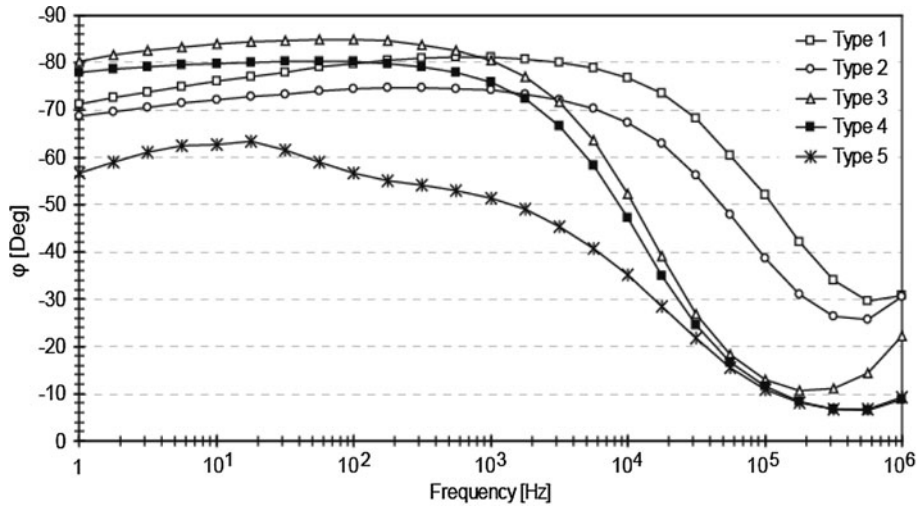

FIGURE 3. Average phase angle (φ) at all measurement frequencies of all new needles sorted by needle type.

composition of the needles. The results from the back scattering are given in Table 3.

Figures 4, 5, 6, 7, and 8 show images at 1000× magnification to illustrate the shape of the needle tip, and 15,000× to get an overview of the surface structure of the active electrode area.

After Treatment

The response for each needle type to different treatments and storage in saline is given in Table 4. The saline (tissue) properties are easiest seen in the HF range of our measurements, so the frequencies above 10 kHz are very important in our application. But since we are here using a saline model with known resistivity[5] for investigating electrode properties, we have chosen to reduce the data set by focusing on 1 Hz and 10 kHz. At these frequencies the differences in electrode properties are more prominent. For frequencies around 10 kHz we have a transition zone

TABLE 3. Alloy composition for each needle type, determined by SEM in back scattering mode.

	Normalized weight distribution (%)		
Needle type	Fe	Cr	Ni
1	71.4	20.6	8.0
2	71.8	20.7	7.5
3	70.6	20.8	8.6
4	71.4	21.2	7.4
5	70.6	21.4	8.0

The measurement focused on the main components and is normalized to 100%. (Purity variables given in maximal concentration in the MGSS tables were not counted in the measurement.)

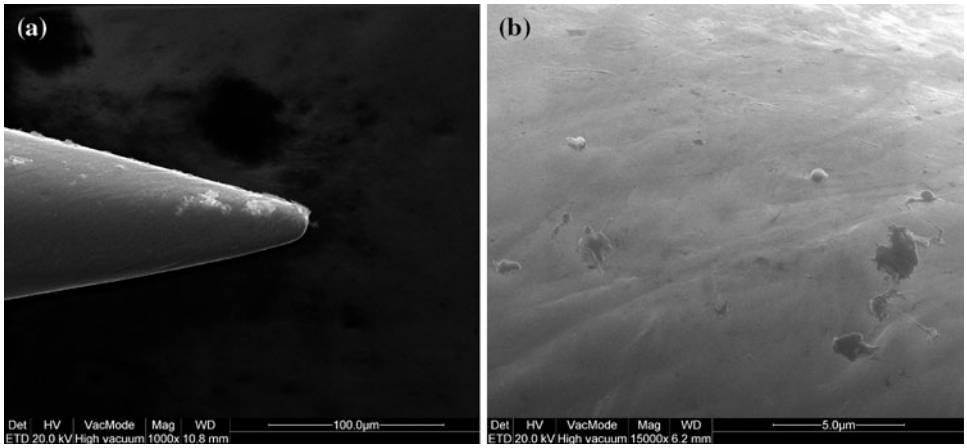

FIGURE 4. Needle type 1.

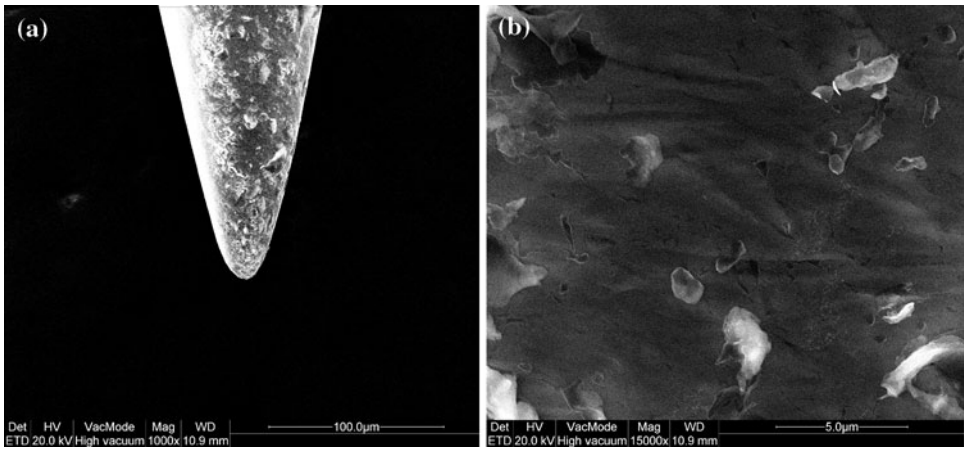

FIGURE 5. Needle type 2.

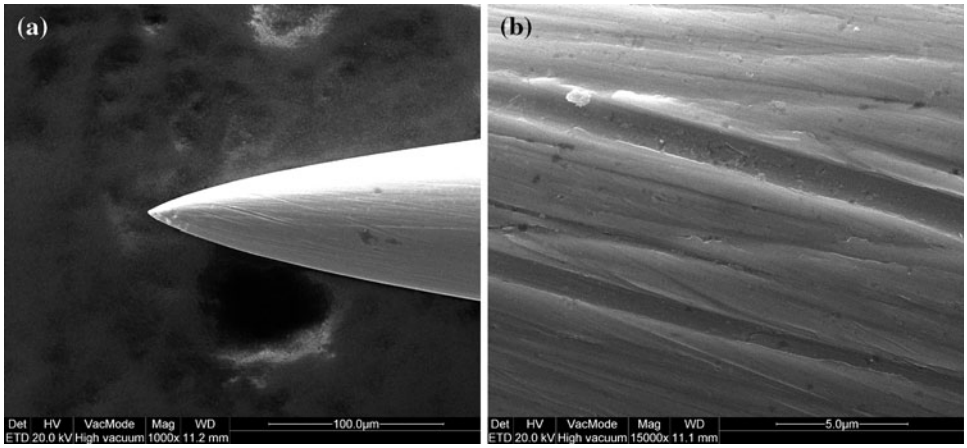

FIGURE 6. Needle type 3.

where the dominance of the measurements goes from EPI to saline (Figs. 2 and 3) or tissue,[15] and at our lowest frequency (1 Hz) we have the total dominance of EPI.

DISCUSSION

The results presented in this study revealed large differences in properties between the investigated

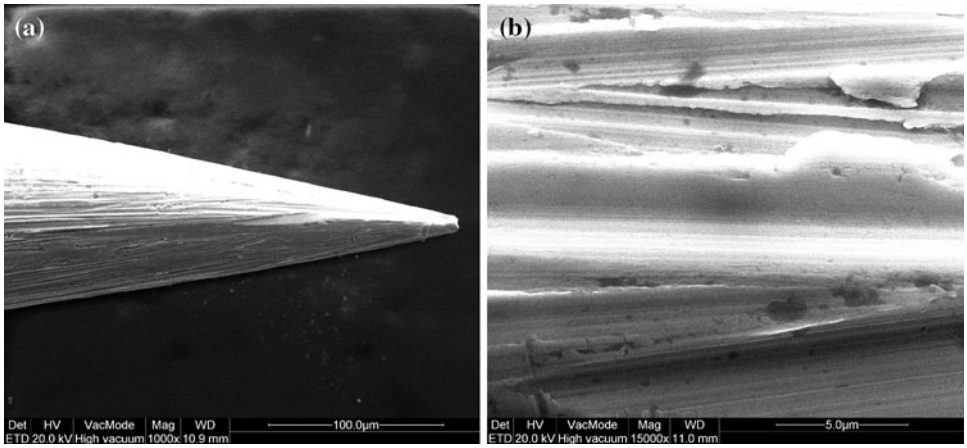

FIGURE 7. Needle type 4.

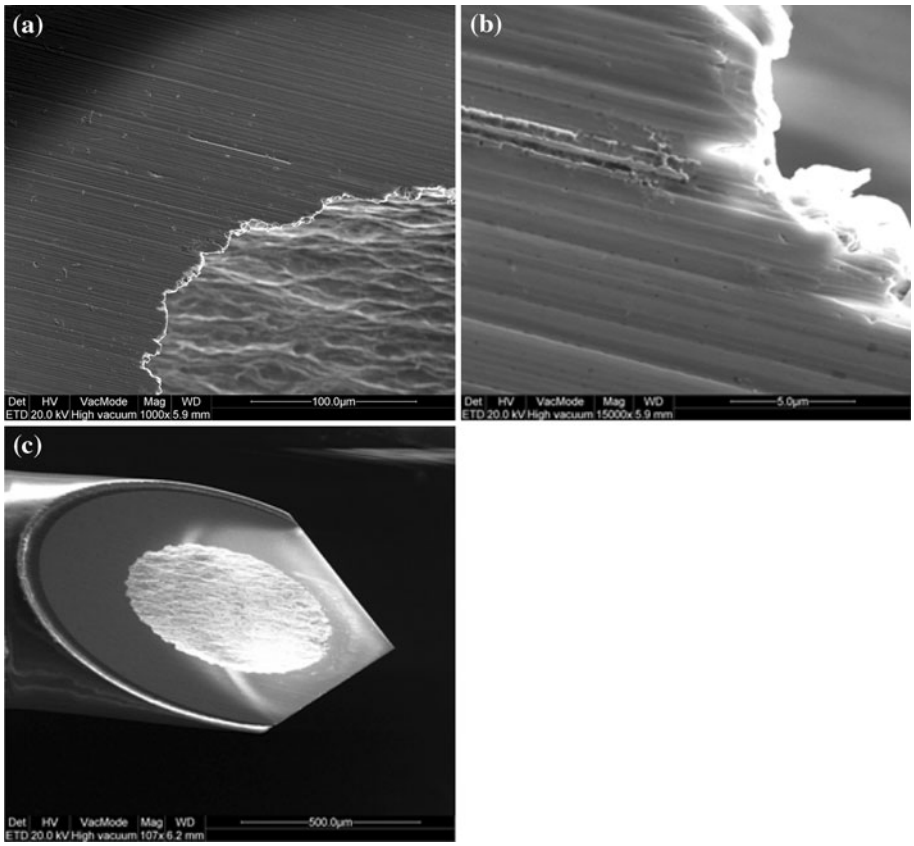

FIGURE 8. Needle type 5. Due to the deviant shape of this needle type we include an image of approx. 100× magnifications for better overview of the needle tip shape.

needle types. This applied both for new needles, and in how they responded to electrolytic treatment and long-term exposure to saline. Our conclusions are based on analyzes of these results in the context of our hypothesis.

New Needles

As described earlier the electrode sizes (Table 1) were chosen for optimal sensitivity. The active electrode areas were from 0.28 mm^2 to about 0.75 mm^2. Needle

TABLE 4. Measured modulus (|Z|, Ω) and phase angle (φ, Deg) during treatment for all needles sorted by type of needle and treatment.

		New				After treatment				5 h in saline				24 h in saline				48 h in saline			
		1 Hz		10 kHz		1 Hz		10 kHz		1 Hz		10 kHz		1 Hz		10 kHz		1 Hz		10 kHz	
Needle	Group	|Z|	φ	|Z|	φ	|Z|	φ	|Z|	φ	|Z|	φ	|Z|	φ	|Z|	φ	|Z|	φ	|Z|	φ	|Z|	φ
Type 1	−3	8.18 M	−71	4.05 k	−76	1.23 M	−66	1.30 k	−52	2.12 M	−76	2.68 k	−47	2.59 M	−74	3.81 k	−55	2.95 M	−71	5.35 k	−60
	−2	7.39 M	−70	3.82 k	−76	1.28 M	−67	1.55 k	−52	2.13 M	−74	3.06 k	−52	2.76 M	−70	5.60 k	−61	3.23 M	−67	6.85 k	−65
	−1	9.78 M	−70	4.35 k	−79	1.68 M	−67	2.58 k	−55	2.86 M	−71	4.81 k	−54	3.,47 M	−67	7.51 k	−61	4.11 M	−64	8.49 k	−67
	0	9.55 M	−74	3.37 k	−78					4.41 M	−70	6.00 k	−71	5.94 M	−60	7.92 k	−75	6.54 M	−57	10.2 k	−78
	1	6.08 M	−73	2.75 k	−75	2.53 M	−70	1.23 k	−57	3.60 M	−66	6.37 k	−67	4.12 M	−64	7.16 k	−70	4.61 M	−62	8.26 k	−72
	2	8.00 M	−70	3.80 k	−76	2.69 M	−68	1.42 k	−58	3.87 M	−66	6.67 k	−66	4.55 M	−63	8.72 k	−71	4.93 M	−62	8.68 k	−72
	3	6.14 M	−71	2.72 k	−76	2.37 M	−67	1.35 k	−57	3.33 M	−66	6.04 k	−64	4.25 M	−61	8.51 k	−69	4.63 M	−60	9.22 k	−71
Type 2	−3	3.35 M	−70	2.06 k	−68	860 k	−70	757	−41	1.30 M	−77	1.01 k	−44	1.28 M	−74	1.37 k	−48	1.30 M	−73	1.58 k	−50
	−2	**2.96 M**	**−71**	**1.55 k**	**−65**	952 k	−66	1.30 k	−46	1.50 M	−74	1.77 k	−45	1.54 M	−72	2.65 k	−49	1.53 M	−70	3.17 k	−52
	−1	3.30 M	−69	2.35 k	−66	1.13 M	−64	1.71 k	−50	1.68 M	−71	2.35 k	−48	1.75 M	−68	3.13 k	−53	1.80 M	−66	3.96 k	−55
	0	3.15 M	−68	2.49 k	−66					3.13 M	−61	4.35 k	−71	3.48 M	−57	5.00 k	−72	2.89 M	−56	4.34 k	−70
	1	3.45 M	−70	1.97 k	−67	1.65 M	−71	1.55 k	−56	1.89 M	−67	3.27 k	−61	1.91 M	−64	3.84 k	−62	1.89 M	−62	4.08 k	−63
	2	**4.81 M**	**−67**	**3.30 k**	**−70**	2.02 M	−69	2.04 k	−59	2.39 M	−68	3.26 k	−60	2.30 M	−65	4.04 k	−62	2.33 M	−62	4.74 k	−63
	3	2.83 M	−70	2.08 k	−61	1.66 M	−71	1.83 k	−57	1.91 M	−68	3.47 k	−60	1.89 M	−65	4.14 k	−63	1.98 M	−63	4.68 k	−64
Type 3	−3	2.61 M	−81	561	−52	773 k	−63	447	−36	1.08 M	−74	817	−56	1.28 M	−73	1.03 k	−59	1.40 M	−71	1.25 k	−62
	−2	2.81 M	−80	606	−52	926 k	−66	509	−39	1.62 M	−74	1.02 k	−60	1.92 M	−72	1.27 k	−63	2.08 M	−71	1.45 k	−64
	−1	2.42 M	−80	550	−52	1.35 M	−78	542	−44	2.61 M	−71	1.60 k	−65	2.95 M	−69	1.98 k	−67	3.26 M	−66	2.62 k	−69
	0	1.84 M	−80	449	−47					2.54 M	−74	1.02 k	−66	2.89 M	−69	1.38 k	−68	3.44 M	−68	1.57 k	−70
	1	2.60 M	−81	550	−52	2.52 M	−80	688	−55	3.08 M	−77	1.08 k	−65	3.26 M	−73	1.39 k	−67	2.41 M	−41	1.59 k	−69
	2	3.04 M	−80	683	−54	2.69 M	−64	979	−58	3.89 M	−75	1.48 k	−66	4.54 M	−71	2.22 k	−70	4.73 M	−69	2.67 k	−71
	3	2.82 M	−81	605	−53	2.35 M	−71	1.10 k	−60	4.31 M	−71	2.37 k	−70	5.34 M	−68	2.92 k	−72	5.50 M	−64	3.64 k	−73
Type 4	−3	802 k	−78	363	−46	342 k	−73	243	−26	338 k	−76	341	−31	378 k	−75	397	−33	390 k	−76	420	−35
	−2	721 k	−78	276	−44	355 k	−80	196	−24	327 k	−78	216	−30	347 k	−80	235	−30	334 k	−79	239	−31
	−1	730 k	−77	308	−48	328 k	−78	205	−26	290 k	−73	208	−27	334 k	−80	224	−27	339 k	−80	228	−29
	0	797 k	−78	315	−48					306 k	−75	225	−30	334 k	−80	232	−28	345 k	−79	237	−30
	1	703 k	−76	304	−48	251 k	−55	221	−30	288 k	−77	196	−22	372 k	−81	226	−27	349 k	−78	229	−28
	2	864 k	−79	306	−48	274 k	−58	222	−29	305 k	−78	205	−24	371 k	−80	243	−29	380 k	−77	248	−31
	3	741 k	−78	278	−45	266 k	−59	209	−25	300 k	−76	194	−22	364 k	−82	228	−27	380 k	−81	232	−29
Type 5	−3	**185 k**	**−55**	435	−34	85,2 k	−51	356	−31	80.9 k	−53	433	−34	65.2 k	−51	491	−35	61.9 k	−45	514	−35
	−2	58.7 k	−42	525	−36	54,5 k	−44	432	−32	59.7 k	−44	629	−32	62.1 k	−44	681	−33	62.2 k	−44	702	−33
	−1	156 k	−59	425	−37	117 k	−62	370	−32	132 k	−62	464	−35	89.1 k	−56	501	−36	90.8 k	−54	517	−36
	0	88.2 k	−58	448	−38					108 k	−61	471	−37	55.9 k	−49	527	−37	56.8 k	−45	525	−37
	1	115 k	−52	391	−34	57.1 k	−40	426	−33	56.4 k	−43	492	−34	60.1 k	−43	563	−35	80.8 k	−47	575	−36
	2	92.2 k	−46	388	−32	105 k	−57	409	−33	87.9 k	−52	449	−35	84.9 k	−52	495	−36	60.4 k	−45	510	−36
	3	119 k	−65	412	−34	76.9 k	−63	474	−34	80.8 k	−57	559	−36	71.5 k	−43	614	−37	74.7 k	−42	624	−37

All numbers are average of three needles in each group, except for the bold numbers that are average of two needles (further explained in the text).

types 4 and 5 had considerably larger active electrode area than types 1, 2, and 3. But as seen in Fig. 2 the impedance properties did not univocally reflect this. The needles with comparable size (types 1–3) showed up to 10-fold differences in resistance at 1 Hz, and the difference from smallest (type 3) to the larger needle electrodes (types 4 and 5) was not very pronounced. (Resistance is not tabulated, but can be calculated from the modulus and phase in Table 4. For needle type 1 resistance and reactance specters are plotted in Kalvøy *et al.*[16]) Our results are in accordance with Wiechers *et al.*[27] They measured $|Z| = 1380$ kΩ at 10 Hz on a needle of same brand as our type 3. Our measurement (Fig. 2) gave an average modulus at 10 Hz of approx. 300 kΩ for this needle type. With a difference in electrode area of approx. four times, this was not far from what we could expect. To determine the active electrode area they used a current excitation to create bubbles on the surface of their electrodes. They also found a 0.95% decreased modulus (69.7 kΩ) after "soaking" in saline containing a wetting agent. Since they do not describe the type of wetting agent nor the time or amplitude of their current excitations, a further discussion of their results in our context is not done.

At high frequencies we expected the electrodes to behave more like ideal electrodes. By ideal we here meant an electrode that transfers a measurement current lossless into the tissue, not interfered by EPI or the uneven current density caused by sharp edges on the active electrode area. If this was the case the impedance would be defined by the purely resistive properties of the saline[5] and the geometry of the electrode, and our HF hypothesis would be confirmed.

For some simplified cases the relation between R and electrode size can be found analytically. By approximating the active electrode to an ellipsoid of revolution model, the resistance (R) of the needle tip inserted from the surface is given by Grimnes and Martinsen[11]:

$$R = \frac{\rho}{2\pi}\frac{\ln\frac{4L}{d}}{L} \quad (L \gg d) \tag{1}$$

where d is the diameter, L is the length of the tip (half long axis), and in our case ρ is the resistivity of the saline. If the model is a whole ellipsoid deep into an infinite volume conductor, the value of R is halved. Our setup was a half ellipsoid deep into a large conductor. Hence, the correct R will probably be something in-between the two models. Since our aim here was comparison of needle types through relative ratios of R, all constants would cancel and the equation above most probably could give us a reasonable estimate.

Needle types 1, 2, and 3 had almost similar active electrode areas (Table 1). The average modulus at 1 MHz was between 290 and 333 Ω (Table 2) and there were no significant differences ($p = 0.05$–0.9) for these needle types. As expected the larger electrodes (types 4 and 5) had lower impedance modulus at 1 MHz (Table 2) (significance $p < 0.001$). Figure 3 shows that the phase shift was noticeably higher at HF for needle types 1 and 2, compared to the others. In a t-test we found that the reactance (X) was the factor with largest differences between needle types and R is the factor with least differences.

Needle types 1, 3, and 4 have a diameter of approx. 0.35 mm (Table 1). The length of the tip is not given, but from visual inspection in microscope the length is measured to approximately 0.6 mm for needle types 1 and 3, and 1.3 mm for type 4. Insertion in Eq. (1) gives an expected resistance ratio (r) between type 1 (or 3) and type 4 of $r = 1.55$. The average measured R at 1 MHz (calculated from Z and φ in Table 2) for needle type 4 was 171 Ω and the average of types 1 and 3 was almost the same at approximately 268 Ω. This gave the ratio 1.57 which was close to the expected. These rough estimates confirmed the hypothesized relationship between the electrode geometry and measured resistance at 1 MHz in saline, but the large phase shift (φ in Table 2) revealed a higher influence from the reactance component than expected. Figures 2 and 3 showed typical patterns for a system of EPI in series with an electrolyte or tissue.[2] The EPI in such a setup is commonly modeled by an element according to Fricke's law,[7,26] with a relatively large phase shift that was reduced as the frequencies increased into the range that was dominated by the resistivity of the saline. For needle types 3, 4, and 5 the phase shift was reduced to about −10° at some hundred kHz, before the negative phase shift increased again as the frequency increased toward 1 MHz. The increased phase shift could most probably be explained by influence from capacitive current paths through the insulated shaft of the needles[15] and stray capacitances at the highest frequencies. Traces of the same pattern could also be seen for needle types 1 and 2, but the negative phase angle never became smaller than −25°, and the stable level in the modulus that could be expected for saline at HF, was not fully reached in our frequency range.

One interpretation of this can be that the geometrically dependent resistance of the saline dominated R, but the significant differences in X and the large negative phase shift indicate that some of the needles had noticeable influence from EPI even at frequencies up to 1 MHz. As described above, influence from needle insulation and stray capacitances can be expected at frequencies in the MHz range. Hence, a frequency range where we solely could measure the resistivity of the saline, uninfluenced by EPI or stray capacitance, could not be found for some of these needle types.

At lower frequencies the differences for some of the needles were above 10-fold. Even for the needle types 1, 2, and 3, with approximately the same size and shape, the differences were up to 3-fold (Fig. 2). Since these differences were of a larger magnitude and not in accordance with the differences in active electrode area, as discussed for HF above, we concluded that other characteristics and not only the size, made significant contributions to the LF impedance properties of these medical grade stainless steel needle electrodes.

Different electrode properties are seen due to metal type. Mirtaheri *et al.*[21] found up to 10-fold differences in resistance between identically shaped electrodes made of aluminum and medical stainless steel. From our earlier findings of different properties for MGSS electrodes,[15] there was good reason to test the hypothesis that the differences found could be explained from differences in alloy composition. As the MGSS comes in sub-grades and they are defined as compositions within a given percent range of elements, we decided to do our own estimation of alloy composition. Our results in Table 3 gave only about 1% differences in amount of Fe, Cr, and Ni for the used needle types are tabulated in Table 3. The result was much more homogenous than we expected, and we decided to regard the hypothesis as rejected without further discussion of what differences in impedance we could expect within these variations or the accuracy of the measurement.

The EPI is inversely dependent of active electrode area, and in the low frequency range the tissue impedance is buried in EPI, and Fig. 2 shows how the EPI decrease with increasing frequency. Even if the EPI can be shown to be tissue dependent,[15,26] the needle with the largest range of tissue-dominated impedance measurements will probably give the best results in tissue discrimination.

The needle type 3 has a slightly smaller active electrode area than the types 1 and 2. From this we should expect that the needle type 3 had higher impedance than types 1 and 2, but the results in Fig. 2 showed the opposite. The modulus at 10 kHz (Table 3) was four times higher for the average of needle type 2 compared to the average of type 3, and the average of needle type 1 was even higher than type 2. This could be due to poor correlation between the real electrode area and the area given by one or both manufacturers, or by other differences in surface properties. Both producers said that no specific surface treatment was done. Even if the difference is not due to electrode material, the microstructure of the electrode surface, sterilization,[19] and other processes that the electrode is exposed to, can cause differences in impedance properties. The structure of the electrode surface is often described in terms of roughness factor,[1] or differences in the real (fractal) area vs. the macrogeometrical area of the electrode (Brummer and Turner[1]; Merrill, p. 186[20]). The SEM images in Figs. 4–8 show needle shapes at 1000× magnification and the surface structure at 15,000× magnification for the needle types used.

As seen in the images there were large variations in surface roughness among the needle types. The only difference between needle types 1 and 2, from the same manufacturer, was that needle type 2 seemed to have more impurities than type 1. Since only one randomly picked sample was investigated, this could only be occasional or just due to a different production batch. Needle type 3 had small groves as if they were ground. Non-exact quantization of the difference in surface area between the needle types were done, but from visual inspection of the SEM-pictures we concluded that the differences between needle types 1, 2, and 3, constituted less than a doubling of the real surface area. Hence, the surface structure could not sufficiently explain the differences in impedance modulus of up to above 3-fold, which was seen for these needle types in Table 4 and Figs. 2 and 3.

The geometrical area of needle type 4 was almost the twice that of needle types 1, 2, and 3 (Table 1), and Fig. 7 showed that needle type 4 had a much higher roughness factor than these needle types. Compared to types 1, 2, and 3 we could expect much lower measured impedance for this type, caused by the high-real electrode area. Compared to types 1 and 2 the difference was about what we could expect (Table 4), both new needles, after treatment and after saline exposure, both at 1 Hz and 10 kHz. But for new needles at 10 kHz the modulus of type 4 was approx. the half of type 3. This difference was much less than expected, and indicates that factors not discovered by the methods of this study, have important influence on the electrode properties. After saline exposure the impedance of needle type 3 drifted and the differences increased to a level more like the expected. From these findings we must expect that differences due to oxidization or other chemical processes also contribute to the measured differences.

Figure 8c shows that needle type 5 is hollow, and in the lower right corner of Fig. 8a and the upper right corner of Fig. 8b, we can see that the inside is uninsulated and has a very high roughness factor. This uninsulated inside of the needle will constitute an enlargement of the active electrode area, but the saline on the inside of the cannula gives gradually increased series resistance to the areas situated further into the cannula. This will give a distributed shielding and most probably constant phase properties for this area. We suggest this as the most important

contributor to the low phase shift seen at LF in Fig. 3 for this needle type.

Treatment

DC stimulation using a large current is efficient for transferring a significant amount of charge in short time, but if the current density is too high reduction of the aqueous solution and bubbles will occur at the electrode surface. In pilot tests we obtained sufficient charge transfer without development of bubbles by using 1 μA stimulation current. In Table 4 we found large differences between the needle types after electrolytic treatment and long-term exposure to saline. The needle type 1 had highest impedance modulus as new, both at 1 Hz and 10 kHz. All needle types had decreased impedance after cathodic treatment (groups −1, −2, and −3). Types 1 and 2 also had a large reduction in modulus after anodic treatment (groups 1, 2, and 3), but the resulting impedance was about double compared to the cathodic. Type 4 was the only type with lowest modulus after anodic treatment. Needle types 3 and 5 had only minor response to the electrolytic treatment, with a small reduction of the impedance after cathodic treatment (both at 10 kHz and 1 Hz, but smallest at 10 Hz). The anodic treatment surprisingly gave increased impedance at 10 kHz; which is the opposite of what we found for the other needle types.

Needle type 4 was the most stabile after saline exposure. Except for a decreased modulus for group 0 after 5 h in saline, there was no significant drift in impedance properties for this needle type. Group 0 of needle type 1 also had a decreased modulus after 5 h in saline, but the rest of the groups (type 1) had unchanged or increased impedance after 5 h. Despite of an approx. 50% increase in the average modulus at 10 kHz for needle type 5 after 48 h, this type had quite stable properties. The modulus for needle types 1, 2, and 3 increased during all three exposure periods and ended up at about the twice or higher after 48 h, both for 1 Hz and 10 kHz. The cathodic treated groups (−1, −2, and −3) had significantly lower modulus after 48 h than the anodic treated groups (1, 2, and 3). The low modulus of group −3 and the high modulus of group 3, indicates that the time of the treatment was significant. A summary of these findings can only be that MGSS needles respond very differently to electrolytic treatment or saline exposure, and that each type of such electrodes should be properly tested if reproducible results of high quality are needed.

For further development of our application we ended with needle type 3, due to the favorable combination of impedance properties and spatial sensitivity. Needle types 1, 2, and 3 had active electrode size giving the optimal spatial sensitivity for our application,[15] and needle types 3, 4, and 5 had the best suited impedance properties. Since impedance measurements require an excitation current, the stability due to flow of current (electrolytic treatment) was seen as a favorable property.

Limitations of the Study

Our measurements were done in saline at room temperature and not in tissue at 37 °C. The measured impedance does not comply directly with what we can expect in a clinical application at body temperature. Temperature drift according to the temperature coefficient of saline and differences in influence on electrode properties between saline and tissue must be considered. For example, exposure to proteins or immunologic responses cannot be modeled in saline.

Short-term processes were not investigated. The shortest period of saline exposure was 5 h. Some of the needle types had about doubled their impedance in this period. Hence, further short-term investigations should be done. Manipulation of electrode surfaces by electrolytic deposition [e.g., silver or platinum (Grimnes and Martinsen, pp. 256–257[11])] are well known processes involving significantly higher current densities than those used in this study. Such methods are relevant for special design of electrodes for further application, but at this stage we have limited the study to commercial electrodes in a saline tissue model using 1 μA current. The interpretation of the results must be based on differences in the local current density during the electrolytic treatment. One micro ampere gives different current density for different active electrode areas.

Needle electrode manufacturers use different methods in production and treatment of their electrodes. We here used SEM to obtain images with high resolution of one randomly picked needle of each type. This was done to get an overview of typical differences in shape and structure to expect from different production methods. Uneven processing or typical variation within same type and brand cannot be found, but such differences are most likely smaller than the differences due to production method. To obtain more quantified details of the surface structure we hope to use an atomic force microscope in further studies, but for an overview of shape and structure the SEM images was seen as sufficient at the present stage.

CONCLUSION

Experimental results showed large variations in the impedance properties of medical grade stainless steel

needle electrodes, both on new needles and as a response to electrolytic treatment or exposure to saline. Our investigations showed that the condition or treatment of the active electrode area is crucial. After electrolytic treatment the EPI decreased. After 5–48 h of saline exposure the EPI increased, both for treated and untreated needles. Cathodic treatment gave lower impedance and drift than anodic or no treatment. Differences in electrode size, roughness or alloy composition cannot alone explain the measured differences. Thus, great care should be taken to obtain reproducible results of high quality. Actual stainless steel electrode types should be properly tested before use. The needle type 3 was best suited for further development of our application.

ACKNOWLEDGMENTS

The authors would like to thank The Centre for Materials Science and Nanotechnology, University of Oslo for excellent assistance during the SEM-scans.

REFERENCES

[1]Brummer, S. B., and M. J. Turner. Electrical stimulation with Pt electrodes: I—A method for determination of "real" electrode areas. *IEEE Trans. Bio. Eng.* 24(5):436–439, 1977.

[2]Bordi, F., C. Cametti, and T. Gili. Reduction of the contribution of electrode polarization effects in the radiowave dielectric measurements of highly conductive biological cell suspensions. *Bioelectrochemistry (Amsterdam Netherlands)* 54(1):53–61, 2001.

[3]Buchthal, F., and A. Rosenfalck. Evoked action potentials and conduction velocity in human sensory nerves. *Brain Res.* 3:1–122, 1966.

[4]Butson, C. R., C. B. Marks, and C. C. McIntyre. Sources and effects of electrode impedance during deep brain stimulation. *Clin. Neurophysiol.* 117:447–454, 2006.

[5]Cooper, R. The electrical properties of salt-water solutions over the frequency range 1–400 Mc/s. *J. Inst. Elect. Eng.* 93:69–75, 1946.

[6]Dorfman, L. J., K. C. McGill, and K. L. Cummins. Electrical properties of commercial concentric EMG electrodes. *Muscle Nerve* 8:1–8, 1985.

[7]Fricke, H. The theory of electrolyte polarization. *Phil. Mag.* 14:310–318, 1932.

[8]Geddes, L. A., C. P. Da Costa, and G. Wise. The impedance of stainless steel electrodes. *Med. Biol. Eng.* 9:511–521, 1971.

[9]Gray, J. R. Conductivity analyzers and their applications. In: Environment Instrumentation and Analysis Handbook, edited by R. D. Down and J. H. Lehr. Wiley, 2004, pp. 491–510.

[10]Grimnes, S. Impedance measurement of individual skin surface electrodes. *Med. Biol. Eng. Comput.* 21:750–755, 1983.

[11]Grimnes, S., and Ø. G. Martinsen. Bioimpedance & Bioelectricity Basics (2nd ed.). San Diego: Academic Press, p. 471, 2008.

[12]Guth, U., V. Winfried, and J. Zosel. Recent developments in electrochemical sensor application and technology—a review. *Meas. Sci. Technol.* 20:1–14, 2009.

[13]Jarzabek, G., and Z. Borkowska. On the real surface area of smooth solid electrodes. *Electrochim. Acta* 42:2915–2918, 1997.

[14]Johnson, M. D., K. J. Otto, J. C. Williams, and D. R. Kipke. Bias voltages at microelectrodes change neural interface properties *in vivo*. In: Proceedings of the 26th Conference IEEE EMBS, 2004, pp. 4103–4106.

[15]Kalvøy, H., L. Frich, S. Grimnes, Ø. G. Martinsen, P. K. Hol, and A. Stubbhaug. Impedance based tissue discrimination for needle guidance. *Physiol. Meas.* 30:129–140, 2009.

[16]Kalvøy, H., B. Nordbotten, C. Tronstad, Ø. G. Martinsen, and S. Grimnes. Impedance properties of stainless steel needle electrodes. *Proc. WC2009 IFMBE* 25:380–383, 2009.

[17]Khambete, N. D., J. Shashidhara, G. S. Bhuvaneshwar, and R. Sivakumar. Impedance measurement system for concentric needle electrodes. In: Proceedings of the RC IEEE-EMBS & 14th, 1995, pp. 1.1–1.2.

[18]Kinouchi, Y., T. Iritani, T. Morimoto, and S. Ohyama. Fast in vivo measurements of local tissue impedances using needle electrodes. *Med. Biol. Eng. Comput.* 35:486–492, 1997.

[19]Ludin, H. P. Electromyography in Practice. Stuttgart-New York: Thieme, 1980.

[20]Merrill, D. R., M. Bikson, and J. G. R. Jeggerys. Invited review. Electrical stimulation of excitable tissue: design of efficacious and safe protocols. *J. Neurosci. Methods* 141:171–198, 2005.

[21]Mirtaheri, P., S. Grimnes, and Ø. G. Martinsen. Electrode polarization impedance in weak NaCl aqueous solutions. *IEEE Trans. Biomed. Eng.* 52:2093–2099, 2005.

[22]Mirtaheri, P., S. Grimnes, Ø. G. Martinsen, and T. I. Tønnessen. A new biomedical sensor for measuring PCO2. *Physiol. Meas.* 25:421–436, 2004.

[23]Sauter, A. R., M. S. Dodgson, H. Kalvøy, S. Grimnes, A. Stubhaug, and Ø. Klaastad. Current threshold for nerve stimulation depends on electrical impedance of the tissue: a study of ultrasound-guided electrical nerve stimulation of the median nerve. *Anesth. Analg.* 108(4):1338–1343, 2009.

[24]Schaldach, M. New aspects in electrostimulation of the heart. *Med. Prog. Technol.* 21:1–16, 1995.

[25]Schwan, H. P. Determination of biological impedances. In: Physical Techniques in Biological Research, Vol. 6, edited by W. L. Nastuk. New York: Academic, 1963, pp. 323–407.

[26]Schwan, H. P. Linear and nonlinear electrode polarization and biological materials. *Ann. Biomed. Eng.* 20:269–288, 1992.

[27]Wiechers, D. O., R. Jeffrey, and W. Richard. EMG needle electrodes: electrical impedance. *Arch. Phys. Med. Rehabil.* 60:364–369, 1979.

[28]Woo, E. J., S. Tungjitkusolmun, H. Cao, J. Z. Tsai, J. G. Webster, V. R. Vorperian, and J. A. Will. A new catheter design using needle electrode for subendocardial RF ablation of ventricular muscles: finite element analysis and in vitro experiments. *IEEE Trans. Biomed. Eng.* 47:23–31, 2000.